Single-cluster Monte Carlo study of the Ising model on two-dimensional random lattices

Wolfhard Janke

Institut für Physik, Johannes Gutenberg-Universität Mainz, 55099 Mainz, Germany

Mohammad Katoot

Department of Physical Sciences, Embry-Riddle Aeronautical University, Daytona Beach, Florida 32114

Ramon Villanova

*Grup de Física Teòrica and Institut de Física d'Altes Energies, Facultat de Ciències,
Universitat Autònoma de Barcelona, 08193 Bellaterra, Spain*

We use the single-cluster Monte Carlo update algorithm to simulate the Ising model on two-dimensional Poissonian random lattices with up to 80 000 sites which are linked together according to the Voronoi-Delaunay prescription. In one set of simulations we use reweighting techniques and finite-size scaling analysis to investigate the critical properties of the model in the very vicinity of the phase transition. In the other set of simulations we study the approach to criticality in the disordered phase, making use of improved estimators for measurements. From both sets of simulations we obtain clear evidence that the critical exponents agree with the exactly known exponents for regular lattices, i.e., that (lattice) universality holds for the two-dimensional Ising model.

I. INTRODUCTION

Physically the concept of random lattices plays an important role in an idealized description of the statistical geometry of random packings of particles.[1-3] A prominent example is the crystallization process in liquids, and many statistical properties of random lattices have been studied in this context.[4] From a more technical point of view, random lattices provide a convenient tool to discretize space without introducing any kind of anisotropy.[5] In the past few years this desirable property of random lattices has been exploited in a great variety of fields. The applications range from quantum field theory or quantum gravity,[5-7] the statistical mechanics of strings or membranes,[8] to the solution of Laplace's equation in the context of diffusion limited aggregation,[9] or the study of growth models for sandpiles,[10] to mention a few. The preserved rotational, or more generally Poincaré, invariance suggests that field theories or spin systems defined on random lattices should reach the continuum or infinite volume limit faster than on regular lattices. An implicit assumption in this approach is that the concept of (lattice) universality, which is known to be true for spin systems on different *regular* lattices, carries over to random lattices. By this, one means that a system defined on different lattice discretizations should exhibit the same qualitative behavior once the physical length scale is much larger than the average lattice spacing. Even though this assumption appears very natural, previous numerical work[11,12] on random lattices could only give weak evidence that it applies in this case as well.

In fact, in view of the equivalence of a random lattice system to a regular lattice system with impurity bonds derived a long time ago,[13] the universality assumption might appear less trivial than naively expected.[14] In particular for the two-dimensional Ising model, according to the Harris criterion,[15] random disorder is marginally important since the critical exponent of the specific heat is $\alpha = 0$. It should be noted, however, that in the random lattice case the equivalent distribution of impurity bonds exhibits complicated correlations, which makes the theoretical analysis even more subtle.

To investigate this point numerically, Espriu *et al.*[12] performed Monte Carlo (MC) simulations of the Ising model on a two-dimensional Poissonian random lattice with $N = 10\,000$ sites, linked together according to the Voronoi-Delaunay prescription.[1-4] Analyzing their data in the high- and low-temperature phase they obtained weak evidence that the critical exponents for the random lattice system agree with the regular Onsager values,[16] which we have summarized for the reader's convenience in Table I. Using a local Metropolis update algorithm as in Ref. 12, it would be very time consuming to obtain a significant improvement, especially in the vicinity of the phase transition where critical slowing down is a severe problem.[17] In the meantime much more efficient update algorithms have been discovered[18-20] which overcome this problem. Together with improved methods of data analysis[21] this now allows one to simulate the model also at criticality with high precision and to study its finite-size scaling (FSS) behavior.[22]

In this paper, we thus present and analyze two sets of extensive simulations of the Ising model on two-dimensional Poissonian random lattices of Voronoi-Delaunay type, varying in size from 5 000 to 80 000 sites.

TABLE I. Exact critical exponents for the regular two-dimensional Ising model.

α	ν	β	γ	η	δ
0(log)	1	0.125	1.75	0.25	15

　　<u>49</u>　9644

In the first set of simulations we concentrate on the very vicinity of the transition point and apply FSS techniques[22] to extract the critical coupling $K_c \equiv 1/k_B T_c$, and the exponents ν, γ/ν, β/ν, and α/ν.[23] The second set of data consists of simulations in the disordered phase for a random lattice of size 40 000 sites. Here we focus on the approach to criticality of the susceptibility and the specific heat, which yield independent estimates of K_c, and the critical exponents γ and α.

To achieve the desired accuracy of the data in reasonable computer time we have applied the single-cluster algorithm[19] to update the spins. In the FSS region we further made extensive use of the reweighting technique,[21] and in the disordered phase we took advantage of the fact that the average cluster size is an improved estimator for the susceptibility.

The paper is divided as follows. In Sec. II, we briefly describe the numerical construction of the random lattice and give a few simulation details. In Sec. III, we present a finite-size scaling analysis of our simulations near the transition point. Section IV is devoted to a discussion of our results in the disordered phase, and in Sec. V we close with a brief summary and a few concluding remarks.

II. THE MODEL AND SIMULATION TECHNIQUES

A. Random lattice construction and properties

In constructing the random lattices we followed closely the method described by Friedberg and Ren.[7] At first we draw N random sites distributed uniformly in a unit square, thereby generating a so called Poissonian distribution. For alternative distributions discussed in the literature see, e.g., Refs. 9 and 24. To link these sites according to the Voronoi-Delaunay prescription, we start by picking one site at random, locate its nearest neighbor, and store this link along with its direction. Next a third site is searched for in a counterclockwise sense by drawing a family of circles that pass through the first two sites

and are centered on their bisector. Once the first triangle is completed this procedure continues with the same steps until all sites are linked. Some care must be exercised when approaching the boundaries of the lattice to ensure the periodic boundary conditions. To implement the nearest-neighbor search efficiently we subdivided the unit square into smaller boxes. The optimal box size is determined by two conflicting requirements. On the one hand, the box size should be large enough to ensure that nearest neighbors will be located with high probability in the same box or at least in the eight surrounding boxes. On the other hand, to minimize the time needed for testing all sites in a box, the box size should be as small as possible. We only performed a "trial and error" optimization based on heuristic arguments, but in any case the complexity of the lattice construction is reduced in this way from order N^2 to order N.

To test our random lattice construction we have measured the average link length $\langle l \rangle$, and the (normalized) distribution of coordination numbers $P(q)$, which can be compared with the exact results given in Refs. 2 and 25. Our results for three different realizations with $N = 10\,000$ sites and one with $N = 80\,000$ sites are collected in Table II. Notice that for $N = 80\,000$ a single site with coordination number $q = 14$ would give $P(14) = 0.000\,012\,5$. Compared with the exact number we thus expect this to happen on the average only every fourth realization. Similarly, a site with $q = 15$ should occur only every 40th realization of a $N = 80\,000$ lattice. The average coordination number $\bar{q}$ was always exactly six, as it should be for periodic boundary conditions (i.e., on a torus) by Euler's theorem, $N - N_L + N_T = \chi$. Here N_L and N_T are the number of links and triangles satisfying $2N_L = 3N_T$, and χ is the Euler characteristic ($=0$ for a torus and $=2$ for a sphere). This implies $\bar{q} = 2N_L/N = 6(1 - \chi/N)$ and thus $\bar{q} = 6$ for the topology of a torus, while for the topology of a sphere there is a correction term $(1 - 2/N)$.

TABLE II. Coordination number distribution $P(q)$ and average link length $\langle l \rangle$ for the three realizations of $N = 10\,000$ and for $N = 80\,000$. The exact numbers for $P(q)$ are taken from Ref. 25, and for $\langle l \rangle = 32/9\pi$ see Ref. 2.

			$P(q)$		
q	$N = 10\,000$	$N = 10\,000$	$N = 10\,000$	$N = 80\,000$	Exact
3	0.0107	0.0112	0.0127	0.010 737 5	0.012 7(8)
4	0.1033	0.1077	0.1090	0.107 962 5	0.107 7(11)
5	0.2535	0.2519	0.2573	0.257 512 5	0.258(2)
6	0.3052	0.3037	0.2923	0.295 250 0	0.294(3)
7	0.2048	0.1991	0.1982	0.200 000 0	0.198(3)
8	0.0889	0.0903	0.0889	0.090 437 5	0.090(20)
9	0.0258	0.0267	0.0313	0.029 750 0	0.028 8(7)
10	0.0068	0.0064	0.0084	0.006 550 0	0.006 95(20)
11	0.0010	0.0026	0.0016	0.001 500 0	0.001 53(9)
12	0.0000	0.0003	0.0002	0.000 275 0	0.000 24(3)
13	0.0000	0.0001	0.0001	0.000 025 0	0.000 029(5)
14	0.0000	0.0000	0.0000	0.000 000 0	0.000 0028(4)
$\langle l \rangle$	1.129 7(32)	1.129 6(33)	1.131 0(33)	1.131 2(12)	1.131 768. . .

B. Model

We use the standard partition function of the Ising model,

$$Z = \sum_{\{s_i\}} e^{-KE} \ , \quad E = -\sum_{\langle ij \rangle} s_i s_j \ , \quad s_i = \pm 1 \ , \tag{1}$$

where $K = J/k_B T > 0$ is the inverse temperature in natural units, and $\langle ij \rangle$ denotes nearest-neighbor links of our two-dimensional random lattices with periodic boundary conditions. In (1) we have adopted the convention of Espriu et al.[12] and assigned each link the same weight.

C. Simulation

It is by now well known that the problem of critical slowing down of local update algorithms at continuous phase transitions can be overcome by nonlocal update algorithms in which whole clusters of spins are flipped in a coherent way.[20] It is intuitively clear that this leads to a much more efficient sampling of long-wavelength fluctuations than in local update schemes. Currently there are two related formulations available: first, the Swendsen-Wang (SW) formulation,[18] in which the whole lattice is decomposed into clusters, and second, Wolff's single-cluster (1C) formulation,[19] which is based on the generation of a single cluster in each step. Various tests of these cluster algorithms, in particular for the Ising model on two- and three-dimensional regular lattices, have clearly demonstrated that critical slowing down is significantly reduced.[26-31] Both formulations are easily implemented on random lattices as well. The only difference is that the coordination number now varies from site to site. In our simulations we have chosen the 1C formulation. This choice was motivated by comparative studies of the two cluster algorithms on regular cubic lattices which favor the 1C formulation. This is very pronounced in three dimensions,[26,31] but also in two dimensions we expect autocorrelation times that are about 2–3 times smaller than for the SW formulation.[26,27]

For the first set of simulations at criticality we generated random lattices with $N = 5000$, $10\,000$, $20\,000$, $40\,000$, and $80\,000$ sites. For later use we adopt the notation for regular lattices and define a linear lattice size L by $L = \sqrt{N}$. To investigate the dependence of thermal averages on different realizations for fixed N, we considered three randomly chosen realizations for $N = 5000$ and $10\,000$, and two for $N = 20\,000$, respectively. All runs were performed at $K_0 = 0.263$, the estimate of K_c as obtained by Espriu et al.[12] From 50 000 to 150 000 clusters were discarded to reach equilibrium from an initially completely disordered state, and a further 4×10^6 clusters were generated for measurements. Every tenth cluster the energy per spin, $e = E/N$, and the magnetization per spin, $m = \sum_i s_i /N$, were measured and recorded in a time series file. The mean cluster size $\langle |C| \rangle$ was obtained from all clusters.

Our second set of data consists of simulations in the disordered phase. Here we used one random lattice with $N = 40\,000$ sites to generate time series for e, m, and $|C|$ at $K = 0.22, 0.225, 0.23, 0.235, 0.24, 0.245, 0.25$, and 0.26,

and another lattice with $N = 80\,000$ sites at $K = 0.252$ and 0.254. The statistics is the same as in the FSS region.

D. Update dynamics

To estimate the autocorrelation time of the measurements of e and $\chi = KNm^2$ we used two methods. First, by measuring the (normalized) autocorrelation function $A(k) = \langle O(k); O(0) \rangle / \langle O(0); O(0) \rangle$ with $\langle O(k); O(0) \rangle \equiv \langle O(k)O(0) \rangle - \langle O(k) \rangle \langle O(0) \rangle$, we computed directly the integrated autocorrelation time $\hat{\tau} = \frac{1}{2} + \sum_{k=1} A(k)$, using a self-consistent upper cutoff[32] of $k_{\max} = 6\hat{\tau}$. For a rough error estimate we used the a priori formula[32] $\epsilon_{\hat{\tau}} = \sqrt{2(2k_{\max} + 1)/N_m}\,\hat{\tau}$, where N_m is the number of measurements. Second, we used the fact that $\hat{\tau}$ enters the error estimate $\epsilon^2 = \sigma^2 2\hat{\tau}/N_m$ for the mean $\bar{O}$ of N_m correlated measurements of variance $\sigma^2 = \langle O; O \rangle$, and determined ϵ^2 by blocking procedures. Using 8000 blocks of 50 measurements each we obtained agreement with the direct method at a 1–2 % level. For a smaller number of blocks (3200 or 800), we observed a clear increase of the fluctuations around the directly obtained values of $\hat{\tau}$ consistent with an inverse square root behavior. Our results are compiled in Table III. We see that the integrated autocorrelation times of the measurements of e and χ are of the order of $\hat{\tau}_e \approx 0.8 – 1.3$ and $\hat{\tau}_\chi \approx 0.7 – 0.9$. Since completely uncorrelated data would give $\hat{\tau} = 0.5$, our sample thus effectively consists of about 200 000 uncorrelated measurements.

While this properly characterizes the statistics of our simulations, the numbers for $\hat{\tau}$ of a single-cluster simulation are not yet well suited for a comparison with other update algorithms or even single-cluster simulations on regular lattices. To get a comparative work estimate, the usual procedure[19] is to convert the $\hat{\tau}$ by multiplying with a factor $f = 10 \langle |C| \rangle / N$ (≈ 3 in our case) to a scale where measurements are taken after every spin has been flipped once (similar to, e.g., Metropolis simulations). In our case, however, the measured $\hat{\tau}$'s are too small to justify this simple rescaling procedure, since nonlinearities caused by the discreteness of MC time would lead to quite severe overestimates. This follows by observing that $A(k)$ is in general a convex function and that $\hat{\tau}$ can be interpreted as the trapezoidal approximation of the area under this curve. Increasing the interval between measurements by a factor of 5 or 10, say, corresponds to measuring only every fifth or tenth point of the curve one would get by taking measurements every iteration. If at the scale of the less frequent measurements $\hat{\tau} \approx 1$, then the trapezoidal approximation becomes obviously poor and overestimates the true area. To see this more explicitly we adopt the usual assumption that the autocorrelation function can be written as a sum of exponentials, $A(k) = \sum_n a_n \exp(-k/\hat{\tau}_n)$, with exponential autocorrelation times $\hat{\tau}_n$ and amplitudes a_n satisfying $\sum_n a_n = A(0) = 1$. Each exponential contributes to $\hat{\tau}$ a term

$$\tfrac{1}{2} a_n \coth(1/2\hat{\tau}_n) = a_n \hat{\tau}_n [1 + 1/12\hat{\tau}_n^2 + \cdots] \ .$$

While the $\hat{\tau}_n$ do get simply rescaled when changing the

TABLE III. Integrated autocorrelation times of energy and susceptibility at the simulation point $K_0=0.263$ ($\approx K_c$). The $\hat{\tau}^{bl}$ follow from an error analysis using 8000 blocks of 50 measurements each, while $\hat{\tau}$ is estimated directly from the autocorrelation function.

N	$\hat{\tau}_e^{bl}$	$\hat{\tau}_e$	$\hat{\tau}_\chi^{bl}$	$\hat{\tau}_\chi$	$\langle|C|\rangle$	f	τ_e	τ_χ
5 000	0.79	0.79(1)	0.67	0.68(1)	1 564.3(1.2)	3.13	2.04(2)	1.54(2)
5 000	0.76	0.76(1)	0.67	0.67(1)	1 642.7(1.1)	3.29	2.02(2)	1.57(2)
5 000	0.78	0.78(1)	0.70	0.68(1)	1 621.0(1.1)	3.24	2.05(2)	1.58(2)
10 000	0.93	0.94(1)	0.74	0.75(1)	2 761.2(2.3)	2.76	2.27(2)	1.54(2)
10 000	0.85	0.86(1)	0.71	0.71(1)	2 992.5(2.3)	2.99	2.14(2)	1.57(2)
10 000	0.80	0.80(1)	0.70	0.69(1)	3 163.6(2.2)	3.16	2.12(2)	1.47(2)
20 000	0.92	0.92(1)	0.78	0.77(1)	5 743.7(4.8)	2.87	2.31(2)	1.68(2)
20 000	0.92	0.94(1)	0.75	0.76(1)	5 666.3(4.2)	2.83	2.34(2)	1.69(2)
40 000	1.04	1.06(1)	0.82	0.82(1)	10 693.7(8.1)	2.67	2.54(3)	1.64(2)
80 000	1.26	1.28(2)	0.93	0.92(1)	18 810.0(18)	2.35	2.80(3)	1.78(2)

measurement interval, the nonlinear relationship with $\hat{\tau}$ clearly shows that such a simple procedure cannot work for integrated autocorrelation times of the order unity.

To circumvent this problem we used the following method. We first performed fits to the ansatz

$$A(k)=a \exp(-k/\hat{\tau}_0)+(1-a)\exp(-k/\hat{\tau}_1) \ ,$$

and then used this function to sum the integrated autocorrelation time at interpolated k values of spacing $\Delta k = 0.1$. Finally we converted these numbers to the usual "Metropolis" scale. For one realization each of the $N=5000$, 10 000, and 20 000 lattices we have repeated the runs with measurements taken after every cluster flip. This amounts to performing ten times more measurements and thus computing the interpolated values of $A(k)$ directly. On the basis of these tests we are quite sure that the interpolation method gives only small overestimates of the order 1–2 % for the energy and about 5% for the susceptibility, respectively.

To conclude this discussion, when aiming at an accurate determination of autocorrelation times with small systematic errors, it is advantageous to perform many measurements per $\hat{\tau}$. The accuracy of static quantities, however, is hardly improved by more frequent, but strongly correlated measurements. In fact, taking into account the time spent for the measurements, it is usually even more efficient to adjust the interval between measurements such that $\hat{\tau} \approx 1$.

The numbers in Table III obtained in this way are very similar to results for the regular square (sq) lattice.[26,27] If we fit the data for the three largest lattices to a power law, $\tau \propto L^z$, we obtain $\tau_e=0.62(6)L^{0.27(2)}$, and $\tau_\chi=1.2(2)L^{0.07(2)}$, respectively. Of course, we have not enough data points and our lattices are too small to exclude other scaling forms. In particular, we get also very good fits to a logarithmic scaling, $\tau=a+b\ln L$, as claimed for the sq lattice,[26,27,33] but even fits to a linear scaling, $\tau=a+bL$, are satisfactory. Explicitly we obtain from the logarithmic fits $\tau_e=-1.0(3)+0.68(5)\ln L$ and $\tau_\chi=1.1(2)+0.11(4)\ln L$, and from the linear fits

$\tau_e=1.84(5)+0.0034(3)L$ and $\tau_\chi=1.58(4)+0.0006(2)L$. For an illustration see Fig. 1.

E. Observables

From the time series of e and m at $K_0=0.263$ it is straightforward to compute in the FSS region various quantities at nearby values of K_0 by standard reweighting.[21] To estimate the statistical errors, the time-series data was split into 20 bins, which were jackknived[34] to decrease the bias in the analysis of reweighted data.

In this way we determined the temperature dependence of the magnetic fourth-order Binder parameter,[35]

$$U_L(K)=1-\frac{\langle m^4\rangle}{3\langle m^2\rangle^2} \ , \tag{2}$$

whose curves for different lattice sizes $L=\sqrt{N}$ should cross for large L in the unique point (K_c,U^*) (up to
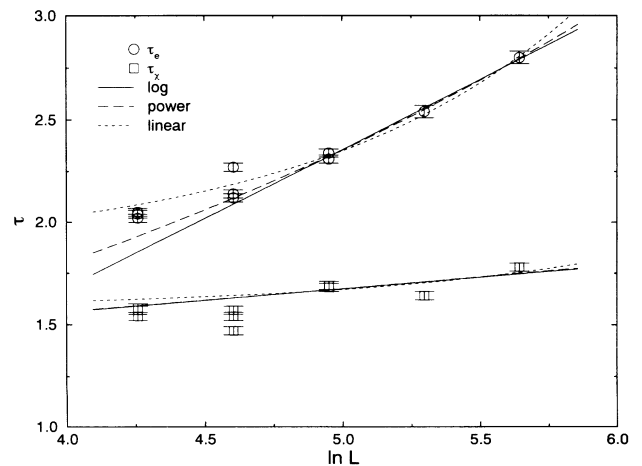

FIG. 1. The autocorrelation times of energy, τ_e, and susceptibility, τ_χ at the simulation point $K_0=0.263$, together with various types of fits to the data of the three largest lattices as discussed in the text.

correction terms). We analyzed the maxima, $\chi'_{\max}$, of the (finite lattice) susceptibility,

$$\chi'(K)=KN(\langle m^2\rangle-\langle|m|\rangle^2) , \tag{3}$$

and studied the (finite lattice) magnetizations at their points of inflection, $\langle|m|\rangle|_{\inf}$. These points follow from the maxima of $d\langle|m|\rangle/dK$, which can be conveniently computed by using the fluctuation formula

$$\frac{d\langle|m|\rangle}{dK}=\langle|m|\rangle\langle E\rangle-\langle|m|E\rangle . \tag{4}$$

Useful scaling information can also be extracted from the logarithmic derivatives[36]

$$\frac{d\ln\langle|m|\rangle}{dK}=\langle E\rangle-\frac{\langle|m|E\rangle}{\langle|m|\rangle} , \tag{5}$$

and

$$\frac{d\ln\langle m^2\rangle}{dK}=\langle E\rangle-\frac{\langle m^2E\rangle}{\langle m^2\rangle} . \tag{6}$$

We further looked at the maxima of the specific heat,

$$C(K)=K^2N(\langle e^2\rangle-\langle e\rangle^2) , \tag{7}$$

and at the minima of the energetic fourth-order parameter

$$V_L(K)=1-\frac{\langle e^4\rangle}{3\langle e^2\rangle^2} . \tag{8}$$

Note that this ratio is usually considered only at first-order phase transitions.[37] As will be demonstrated below, however, it carries useful information at a continuous phase transition as well.

In the simulations in the disordered phase we concentrated on the approach to criticality of the specific heat and the susceptibility, as defined in (3) or, since $\langle m\rangle=0$, more properly as

$$\chi(K)=KN\langle m^2\rangle . \tag{9}$$

For the latter definition an improved estimator is available,[26] being simply the average cluster size,

$$\chi_{\mathrm{imp}}(K)=K\langle|C|\rangle . \tag{10}$$

III. RESULTS IN THE FINITE-SIZE SCALING REGION

In this section we describe the analysis of our data near criticality, using reweighting techniques[21] and FSS ideas.[22]

A. Binder parameter and estimates for K_c, U^*, and ν

It is well known[35] that the $U_L(K)$ curves for different lattice sizes L should intersect around (K_c,U^*) with slopes $U'_L\equiv dU_L/dK\propto L^{1/\nu}$, where U^* is the (universal) "renormalized charge" and ν is the critical exponent of the correlation length. More precisely, due to corrections to the leading FSS behavior, the curves for L and L' should cross in points $K^{\times}=K^{\times}(L,L')$ which approach K_c for large lattice sizes. Our results for $K^{\times}(L,L')$ ob-

tained by reweighting the primary data at $K_0=0.263$ are collected in Table IV. By looking through the table we observe that there are rather strong fluctuations between different replicas for a fixed number of sites N. Even though these fluctuations decrease with increasing N, with the present data it is impossible to apply the standard extrapolation formula[35] for estimating K_c. Hence taking as our final estimate for K_c the average of the five values for $K^{\times}(L,L')$ from the three largest lattices, we obtain

$$K_c=0.2630\pm0.0002 . \tag{11}$$

This value is in good agreement with the estimates in Ref. 12 from high-temperature series expansions $(K_c\approx0.263\,03)$ and MC simulations in the disordered phase $[K_c=0.2631(3)]$. As already noted in Ref. 12 the value for K_c is very close to the exact critical coupling $\ln(3)/4=0.274\,65\ldots$ of the regular triangular lattice whose coordination number is also $q=6$. The (rough) error estimate in (11) should also reflect the fluctuations caused by the different random lattice realizations for fixed N, which in our case are much larger than the statistical errors.

For the same reason, the estimates of U^* in Table IV show stronger fluctuations than our statistics would suggest. Taking the average over all lattice sizes and replicas at our estimate of the critical point, $K_c=0.2630$, we obtain

$$U^*=0.6123\pm0.0025 . \tag{12}$$

The corresponding values at $K=K_c-0.0002$ and $K=K_c+0.0002$ are $U^*=0.6054(25)$ and $U^*=0.6183(28)$, so that taking into account the uncertainties in K_c the error bar in (12) should probably be increased to 0.0070. This then would be consistent with an average over the five lower entries in Table IV, which gives $U^*=0.6176(60)$. Our value for U^* is practically indistinguishable from MC estimates for the regular sq lattice which are $U^*=0.615(10)$ (Ref. 38) and $U^*=0.611(1)$ (Ref. 33). This good agreement may be taken as a first indication of lattice universality.

To extract the critical exponent ν several methods are possible. One would, e.g., analyze the scaling of the slopes $U'_L(K)=dU_L/dK\propto L^{1/\nu}$ at $K=K_c$, or more generally at any sequence of K values for which the scaling variable $x=(K-K_c)L^{1/\nu}$ is constant. Examples are the locations of the specific-heat or susceptibility maxima which are expected to scale as $K_{\max}(L)=K_c+aL^{-1/\nu}$, with a being a constant. Another convenient choice of such a sequence are the points where $U'_L(K)$ is maximal. In this case one gets the desired slopes $U'_{\max}(L)$ directly, without explicit knowledge of the corresponding K values.

We have tried all of these possibilities, but not all gave sensitive results in our case. The errors on U'_L at fixed $K=K_c$ are clearly dominated by the replica fluctuations. Without further simulations to increase the replica statistics it is then impossible to obtain reliable fits. The second, self-consistent method turned out to be much more suited for our problem. With the simplest choice of

TABLE IV. Estimates of $v_{\text{eff}}(L,L')$, $K^{\times}(L,L')$, and $U^* \approx U_L(K^{\times}(L,L'))$ from the magnetic fourth-order Binder parameter for pairs of lattices of size L and L'.

$L\backslash L'$	10 000	10 000	10 000	20 000	20 000	40 000	80 000
5 000	1.008(16)	0.993(17)	1.004(48)	1.002(13)	0.980(14)	1.010(12)	1.0017(45)
	0.263 744(43)	0.262 083(40)	0.260 813(81)	0.262 172(17)	0.262 346(24)	0.262 459(16)	0.262 810 7(67)
	0.617 47(88)	0.581 4(14)	0.541 7(34)	0.583 78(74)	0.588 27(86)	0.591 07(66)	0.599 31(40)
5 000	1.012(20)	1.023(20)	1.039(32)	1.020(11)	1.004(12)	1.017(10)	1.008 3(49)
	0.264 840(29)	0.263 155(23)	0.261 847(46)	0.262 615(13)	0.262 780(16)	0.262 704(10)	0.262 959 2(54)
	0.637 64(33)	0.614 98(46)	0.586 5(14)	0.604 57(38)	0.607 94(41)	0.606 41(32)	0.611 41(21)
5 000	1.012(14)	1.020(13)	1.042(34)	1.017(11)	0.999(12)	1.016 3(97)	1.006 8(41)
	0.264 493(30)	0.262 811(31)	0.261 506(52)	0.262 474(16)	0.262 641(15)	0.262 626(11)	0.262 912 3(49)
	0.632 38(41)	0.605 76(75)	0.573 3(18)	0.598 49(53)	0.602 20(44)	0.601 87(38)	0.607 82(23)
10 000				0.979(95)	0.918(58)	1.047(31)	1.003 9(69)
				0.261 104(10)	0.261 414(66)	0.262 064(27)	0.262 660 3(75)
				0.506 1(64)	0.527 5(39)	0.560 0(14)	0.584 75(55)
10 000				1.011(27)	0.974(22)	1.015(15)	1.002 8(46)
				0.262 237(33)	0.262 527(36)	0.262 572(13)	0.262 928 4(66)
				0.587 1(14)	0.597 1(13)	0.598 53(57)	0.609 07(34)
10 000				1.017(15)	0.997(17)	1.011 1(98)	1.004 5(56)
				0.263 157(27)	0.263 420(27)	0.262 954(12)	0.263 135 1(70)
				0.623 59(70)	0.628 76(62)	0.619 14(42)	0.623 14(28)
20 000						1.010(20)	0.998 4(62)
						0.262 811(20)	0.263 128 9(75)
						0.612 20(83)	0.622 77(31)
20 000						1.055(39)	1.010 6(90)
						0.262 607(29)	0.263 050 2(77)
						0.600 7(15)	0.617 81(39)
40 000							1.002(16)
							0.263 352(15)
							0.634 31(54)

the maxima of U_L', however, we run into the problem that they lie too far away from our simulation point, thus allowing no safe reweighting. Choosing as sequence of K values the locations of the specific-heat or susceptibility maxima, $K_{\text{max}}^C(L)$ or $K_{\text{max}}^{\chi'}(L)$ (see Table V), or the inflection points of the magnetization, $K_{\text{inf}}^{\langle|m|\rangle}(L)$ (see Table VI), we obtain the fits shown in Fig. 2. From the inverse of the slopes we read off

$$v = 1.021 \pm 0.033 \quad (\text{at } K_{\text{max}}^C), \tag{13}$$

$$v = 0.996 \pm 0.028 \quad (\text{at } K_{\text{max}}^{\chi'}), \tag{14}$$

$$v = 1.020 \pm 0.020 \quad (\text{at } K_{\text{inf}}^{\langle|m|\rangle}), \tag{15}$$

TABLE V. Extrema for the (finite lattice) susceptibility (χ'_{max}), the specific heat (C_{max}), and the energy moment ratio (V_{min}), together with their respective pseudocritical couplings.

N	$K_{\text{max}}^{\chi'}$	χ'_{max}	K_{max}^C	C_{max}	K_{min}^V	V_{min}
5 000	0.259 772(39)	42.77(19)	0.262 041(66)	2.010 9(53)	0.260 43(17)	0.664 378(12)
5 000	0.259 305(63)	43.09(29)	0.261 41(12)	2.017(10)	0.259 40(59)	0.664 321(33)
5 000	0.259 448(39)	43.09(18)	0.261 64(11)	2.013 8(71)	0.260 05(22)	0.664 354(22)
10 000	0.260 930(28)	79.27(29)	0.262 421(49)	2.160 0(73)	0.261 532(93)	0.665 459 5(53)
10 000	0.260 446(30)	78.61(34)	0.262 092(78)	2.137 4(68)	0.261 31(11)	0.665 472 0(74)
10 000	0.260 037(48)	78.17(65)	0.261 723(73)	2.134 5(89)	0.260 954(88)	0.665 467 0(81)
20 000	0.260 871(55)	145.2(1.4)	0.262 086(86)	2.276(13)	0.261 60(16)	0.666 034 7(66)
20 000	0.261 023(30)	146.3(1.2)	0.261 98(11)	2.311(18)	0.261 50(14)	0.666 019 9(82)
40 000	0.261 526(33)	259.1(2.5)	0.262 310(84)	2.421(22)	0.262 081(90)	0.666 334 0(43)
80 000	0.261 991(41)	492.2(6.1)	0.262 3(28)	2.600(97)	0.261 49(83)	0.666 481(11)

TABLE VI. Inflection points $K_{\text{inf}}^{\langle|m|\rangle}$ of the magnetization, and $\langle|m|\rangle$ and $d\langle|m|\rangle/dK$ at $K_{\text{inf}}^{\langle|m|\rangle}$. Also given are the extrema of the logarithmic derivatives (5) and (6), and their respective pseudocritical couplings.

N	$K_{\text{inf}}^{\langle|m|\rangle}$	$\langle|m|\rangle\vert_{\text{inf}}$	$\left.\dfrac{d\langle|m|\rangle}{dK}\right\vert_{\text{max}}$	$K_{\text{max}}^{\ln\langle|m|\rangle}$	$\left.\dfrac{d\ln\langle|m|\rangle}{dK}\right\vert_{\text{max}}$	$K_{\text{max}}^{\ln\langle m^2\rangle}$	$\left.\dfrac{d\ln\langle m^2\rangle}{dK}\right\vert_{\text{max}}$
5 000	0.260 943(47)	0.4474(21)	45.73(19)	0.258 59(26)	114.9(1.8)	0.258 11(27)	192.8(2.9)
5 000	0.260 34(10)	0.4377(51)	46.65(44)	0.257 1(12)	124.1(6.7)	0.256 4(12)	211(13)
5 000	0.260 525(71)	0.4409(35)	46.43(31)	0.258 00(42)	119.5(3.2)	0.257 55(42)	200.1(5.4)
10 000	0.261 709(38)	0.4247(23)	62.46(27)	0.260 14(14)	164.9(2.5)	0.259 79(19)	277.2(4.6)
10 000	0.261 298(52)	0.4289(33)	61.76(35)	0.259 87(16)	159.5(3.2)	0.259 55(21)	267.0(5.8)
10 000	0.260 942(44)	0.4293(28)	61.61(51)	0.259 29(29)	160.4(3.3)	0.259 09(24)	266.5(4.8)
10 000	0.260 942(44)	0.4293(28)	61.61(51)	0.259 29(29)	160.4(3.3)	0.259 09(24)	266.5(4.8)
20 000	0.261 499(93)	0.4039(84)	83.7(1.1)	0.258 32(67)	288(57)	0.257 82(72)	485(96)
20 000	0.261 529(62)	0.3985(58)	85.7(1.2)	0.260 38(14)	244.2(8.4)	0.260 14(16)	409(14)
40 000	0.261 979(33)	0.3980(45)	111.5(1.7)	0.261 359(86)	305.8(9.2)	0.261 247(83)	512(15)
80 000	0.262 244(92)	0.359(15)	156.2(2.8)	0.260 98(83)	576(137)	0.260 6(12)	972(276)

in very good agreement with the Onsager value for regular lattices, $v=1$. The quality of the fits, however, is relatively poor.

We therefore used finally yet another approach which is based on the effective exponents

$$v_{\text{eff}} = \frac{\ln(L'/L)}{\ln[U'_{L'}(K^\times)/U'_L(K^\times)]} \ . \tag{16}$$

Our results for v_{eff} are again collected in Table IV and plotted as open circles in Fig. 3, where the x axis corresponds to the 38 possible combinations of L and L'. We see that within the error bars all entries are compatible with $v=1$. The average over all entries gives

$$v = 1.008 \pm 0.022 \quad \text{(effective } v\text{'s)} , \tag{17}$$

where the error estimate is the standard deviation of the v_{eff}. If we take only the nine crossing points of the $N=80\,000$ lattice with all other lattices into account

(filled circles in Fig. 3), then we obtain

$$v = 1.0043 \pm 0.0036 \quad \text{(effective } v\text{'s)} . \tag{18}$$

We can thus conclude that our estimates of the exponent v for random lattices are fully consistent (at a 0.5% level) with the exact regular lattice value of $v=1$.

Assuming $v=1$, we can use the asymptotic FSS behavior of the pseudo-transition points, e.g., $K_{\text{max}}^C(L)=K_c+aL^{-1/v}$, to obtain further estimates of the critical coupling K_c from linear fits in $1/L$. Our results from fits to the data (see Tables V and VI) of the three largest lattices are

$$K_c = 0.262\,95 \pm 0.000\,33 \quad \text{(from } K_{\text{max}}^C\text{)} , \tag{19}$$

$$K_c = 0.262\,947 \pm 0.000\,077 \quad \text{(from } K_{\text{max}}^{\chi'}\text{)} , \tag{20}$$

$$K_c = 0.263\,04 \pm 0.000\,14 \quad \text{(from } K_{\text{inf}}^{\langle|m|\rangle}\text{)} , \tag{21}$$

in good agreement with the estimate (11) based on the Binder parameter intersections.
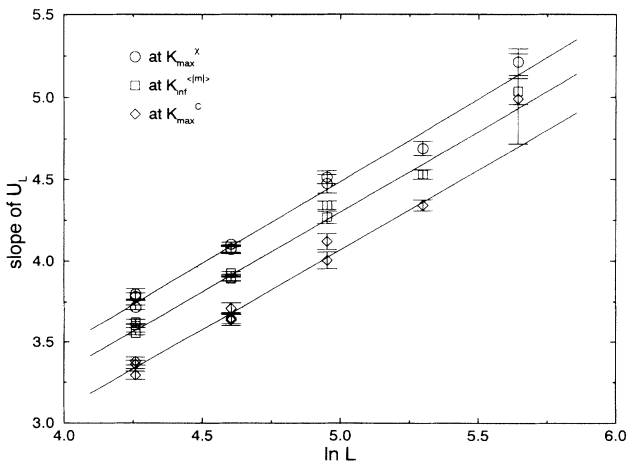

FIG. 2. Finite-size scaling of the Binder parameter slopes at sequences of $K(L)$ values for which the scaling variable $x \equiv [K(L)-K_c]L^{1/v}$ is constant. From the inverse slope of the least-squares fits we obtain estimates of $v=0.996(28)$ $[K(L)=K_{\text{max}}^{\chi'}(L)]$, $v=1.020(20)$ $[K(L)=K_{\text{inf}}^{\langle|m|\rangle}(L)]$, and $v=1.021(33)$ $[K(L)=K_{\text{max}}^C(L)]$, respectively.

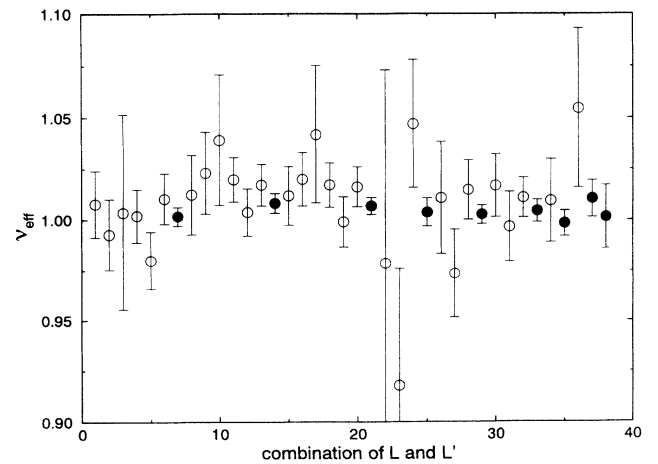FIG. 3. Results for the effective exponents v_{eff} defined in Eq. (16). The x axis labels the 38 possible combinations of lattices of size N and N', starting with 5000/10 000, 5000/20 000, and so on. The filled circles show all possible values for $N'=80\,000$.

B. Susceptibility and γ/ν

To extract the ratio of exponents γ/ν we used that the maxima of the susceptibility should scale for sufficiently large L like

$$\chi'_{max}(L) = \chi'(K^{\chi'}_{max}(L), L) = A L^{\gamma/\nu} . \tag{22}$$

Our results for $K^{\chi'}_{max}$ and χ'_{max} are collected in Table V, and the χ'_{max} are plotted vs L on a log-log scale in Fig. 4. The straight-line fit shown in Fig. 4 gives

$$\gamma/\nu = 1.7503 \pm 0.0059 , \tag{23}$$

with an amplitude $A = 0.02491(67)$, and a goodness-of-fit parameter (Ref. 39) $Q = 0.035$. This is again in excellent agreement with the exact value for the two-dimensional Ising model on a regular lattice, $\gamma/\nu = 1.75$. Even though the Q value of the fit is quite low, we do not see in Fig. 4 any trend with increasing lattice size. In fact, if we discard the data for $N = 5000$, the fit yields $\gamma/\nu = 1.7468(91)$ with $Q = 0.015$, and if we further discard the data for $N = 10\,000$, we obtain $\gamma/\nu = 1.735(19)$ with $Q = 0.005$. Constrained fits with $\gamma/\nu = 1.75$ held fixed at its theoretical value, are equally acceptable and yield for the amplitude $A = 0.024\,938(45)$ with $Q = 0.071$, or, discarding the $N = 5000$ data, $A = 0.024\,952(59)$ with $Q = 0.037$. We can thus conclude that universality also holds as far as γ/ν is concerned.

Notice that in these fits (whether linear or not) it does not matter whether we fit over all ten data points or first compute the weighted replica averages for $N = 5000$, $10\,000$, and $20\,000$ and then fit over five data points. It is easy to show[40] that the results must be identically the same, apart from the Q values. Here and in the following we always quote the Q value for first computing the replica averages.
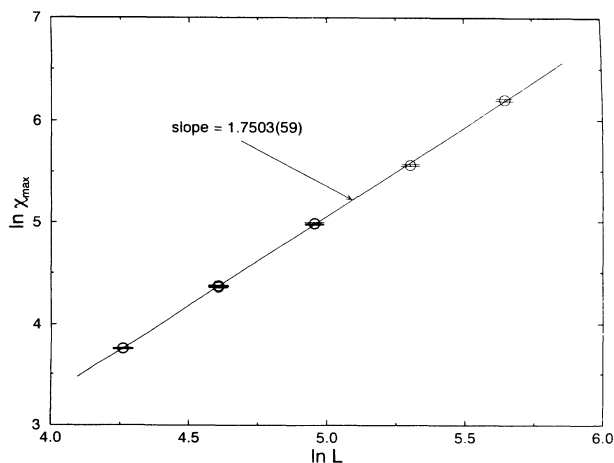
C. Magnetization and β/ν

The standard way to extract the exponent ratio β/ν is to consider the FSS of the magnetization at K_c,

$$\langle |m| \rangle (K_c) \propto L^{-\beta/\nu} . \tag{24}$$

We tried this also here, but due to the replica fluctuations the resulting scaling curve was difficult to analyze. As a solution to this problem we decided to study the scaling behavior of $\langle |m| \rangle$ at the point of inflection, i.e., at the point where $d\langle |m| \rangle /dK$ is maximal. Since these points should scale as usual, $(K^{\langle |m| \rangle}_{inf} - K_c) L^{1/\nu} \equiv tL^{1/\nu} = \text{const}$, we expect

$$\langle |m| \rangle |_{inf} = L^{-\beta/\nu} f(tL^{1/\nu}) \propto L^{-\beta/\nu} , \tag{25}$$

and, since a derivative with respect to K picks up a factor $L^{1/\nu}$ from the argument of the scaling function f,

$$\frac{d\langle |m| \rangle}{dK} \bigg|_{max} = L^{-\beta/\nu + 1/\nu} f'(tL^{1/\nu}) \propto L^{(1-\beta)/\nu} . \tag{26}$$

Consequently, the scaling of the maxima of the logarithmic derivatives (5) and (6) should be given by

$$\frac{d\ln\langle |m| \rangle}{dK} \bigg|_{max} = \frac{d\langle |m| \rangle /dK}{\langle |m| \rangle} \bigg|_{max} \propto L^{1/\nu} , \tag{27}$$

and

$$\frac{d\ln\langle m^2 \rangle}{dK} \bigg|_{max} = \frac{d\langle m^2 \rangle /dK}{\langle m^2 \rangle} \bigg|_{max} \propto L^{1/\nu} , \tag{28}$$

thus providing another means to estimate the correlation length exponent ν.

Our data for these quantities are given in Table VI. The scaling of $\langle |m| \rangle$ at the inflection point is shown in the log-log plot of Fig. 5. The linear fit through all data points gives

$$\beta/\nu = 0.1208 \pm 0.0092 , \tag{29}$$

FIG. 4. Finite-size scaling of the (finite lattice) susceptibility maxima χ'_{max}. The slope of the linear least-squares fit yields $\gamma/\nu = 1.7503(59)$.
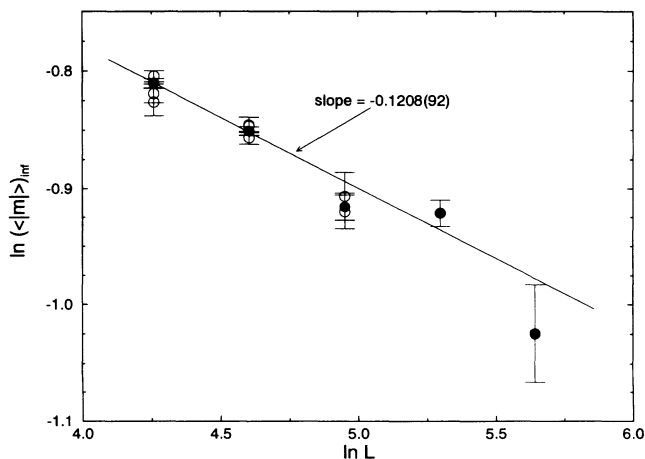

FIG. 5. Finite-size scaling of the (finite lattice) magnetization $\langle |m| \rangle$ at its point of inflection. The filled circles show the replica averages. From the slope of the linear least-squares fit we obtain $\beta/\nu = 0.1208(92)$.

with $Q = 0.10$. This value is again perfectly compatible with the exact result for regular lattices, $\beta/\nu = 0.125$. Omitting the data of the smallest lattice, we obtain $\beta/\nu = 0.122(15)$, with $Q = 0.04$.

The scaling of the maxima of $d\langle |m| \rangle /dK$ is shown in Fig. 6. Here we obtain from the fit

$$(1-\beta)/\nu = 0.8704 \pm 0.0081 \tag{30}$$

with $Q = 0.39$, in agreement with the regular lattice result $(1-\beta)/\nu = 0.875$. Omitting the data of the smallest lattice our estimate even improves to $(1-\beta)/\nu = 0.875(13)$ with $Q = 0.24$.

Finally, using the maxima of the logarithmic derivatives (5) and (6) we obtain two further estimates for ν. From the linear fits in the log-log plots shown in Fig. 7 we read off

$$\nu = 1.037 \pm 0.031 \tag{31}$$

with $Q = 0.06$, and

$$\nu = 1.042 \pm 0.030 \tag{32}$$

with $Q = 0.04$, respectively. The two values for ν are fully consistent with our previous estimates and with the regular lattice result of $\nu = 1$.

D. Specific heat and α/ν

We now turn to the specific heat which is usually the most difficult quantity to analyze. The reason is that, compared to the susceptibility, the critical divergence is much weaker and regular background terms become important. Recalling our result $\nu \approx 1$ and assuming hyperscaling to be valid for the random lattice as well, we expect $\alpha = 2 - d\nu \approx 0$, as for a regular lattice. The corresponding FSS prediction is then

$$C_{max}(L) = C(K^C_{max}(L), L) = B_0 + B_1 \ln L \ . \tag{33}$$

The semilog plot in Fig. 8 clearly demonstrates that our

FIG. 7. Finite-size scaling of the maxima of the logarithmic derivatives $d \ln\langle |m| \rangle /dK$ $(p=1)$ and $d \ln\langle m^2 \rangle /dK$ $(p=2)$. The slopes of the linear least-squares fits are estimates of $1/\nu$, resulting in $\nu = 1.037(31)$ $(p=1)$ and $\nu = 1.042(30)$ $(p=2)$, respectively.

data in Table V are consistent with this prediction. A linear fit through all data points gives $B_0 = 0.346(52)$ and $B_1 = 0.391(12)$ with $Q = 0.84$. It should be remarked, however, that the confirmation of $\alpha = 0(\log)$ is not really conclusive. Due to the small range over which C_{max} varies we can fit the data also with a simple power-law ansatz $C_{max} \propto L^{\alpha/\nu}$, yielding $\alpha/\nu = 0.1824(53)$ with $Q = 0.93$; see Fig. 8. Discarding first only the data points for $N = 5000$ and then also those for $N = 10\,000$, we obtain $\alpha/\nu = 0.180(10)$ with $Q = 0.83$ and $\alpha/\nu = 0.168(27)$ with $Q = 0.72$, respectively. There is thus a small downward trend, but our data is obviously also consistent with a power-law ansatz. We also tried a nonlinear three-parameter fit to the more reasonable ansatz $C_{max} = b_0 + b_1 L^{\alpha/\nu}$. As a result we then obtain an ex-
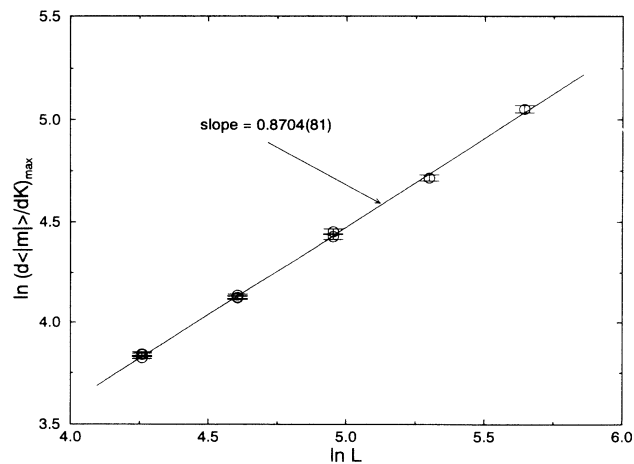

FIG. 6. Finite-size scaling of the maxima of $d\langle |m| \rangle /dK$, used to determine the points of inflection of $\langle |m| \rangle$. The slope of the linear least-squares fit is an estimate for $(1-\beta)/\nu = 0.8704(81)$.
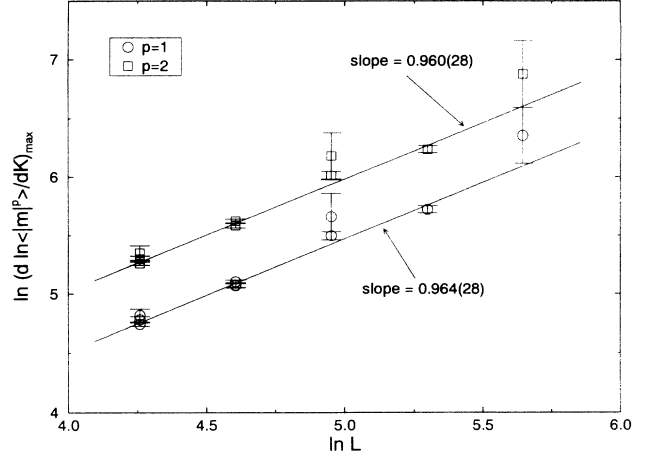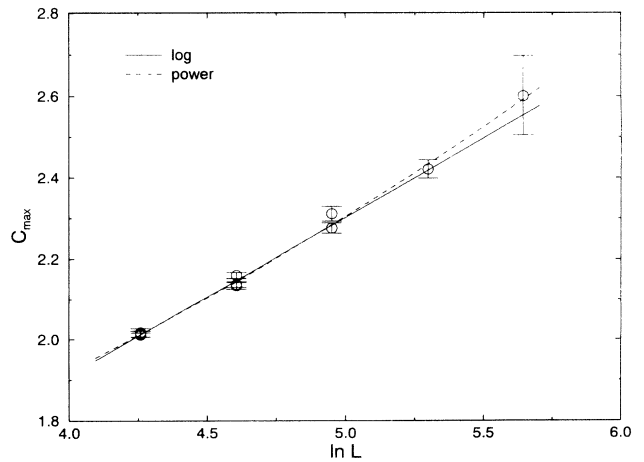

FIG. 8. Finite-size scaling of the specific-heat maxima C_{max}. Also shown are least-squares fits to a logarithmic ansatz, $C_{max} = B_0 + B_1 \ln L$ [with $B_0 = 0.346(52)$, $B_1 = 0.391(12)$], and to a pure power-law ansatz, $C_{max} = cL^{\alpha/\nu}$ [with $c = 0.926(22)$, $\alpha/\nu = 0.1824(53)$].

ponent ratio $\alpha/\nu = 0.17(16)$ consistent with zero, but the errors on all three parameters are much too large to draw a firm conclusion from such a fit.

To convince ourselves that these problems are not a special property of random lattices, we have compared our results with similar fits for the Ising model on a regular sq lattice, employing its known analytical solution for $L \times L$ lattices with periodic boundary conditions.[41] The results for K_{max}^C and C_{max} for various L are collected in Table VII. The values of L that roughly correspond to our random lattice sizes are $L = 80$, 100, 140, 200, and 280. If we fit the corresponding five values of C_{max} to the ansatz (33), we obtain $B_0 = 0.1831$ and $B_1 = 0.4976$, in reasonable agreement with the exact results[41] $B_0 = 0.201359\ldots$ and $B_1 = 8K_c^2/\pi = 2[\ln(1 + \sqrt{2})]^2/\pi = 0.494358\ldots$. The small discrepancies can be attributed to the neglected correction terms of the type $B_2 L^{-1}\ln L + B_3 L^{-1}$. While $B_2 = \frac{3}{2}\sqrt{2}B_1 \times 0.31775 = 0.333222$ is also known analytically, B_3 has not been worked out explicitly. Using all data in Table VII and keeping the parameters B_0, B_1, and B_2 fixed at their theoretical values, we estimate numerically $B_3 \approx -2$. If we try to fit the regular lattice data for $L = 80, \ldots, 280$ to a power law $L^{\alpha/\nu}$ (which is definitely *wrong* in this case), we obtain $\alpha/\nu = 0.1941$, i.e., a value of roughly the same size as for the corresponding random lattice fit.

E. Energy cumulant

We also looked at the fourth-moment parameter $V_L(K)$ defined in (8), involving the energy moments. By rewriting V_L as

$$V_L = 1 - \frac{1}{3}\frac{1 + 6\langle \delta e^2 \rangle + 4\langle \delta e^3 \rangle + \langle \delta e^4 \rangle}{1 + 2\langle \delta e^2 \rangle + \langle \delta e^2 \rangle^2}, \quad (34)$$

with $\delta e \equiv (e - \langle e \rangle)/\langle e \rangle$, it is easy to see that in leading order

$$V_L \sim \frac{2}{3} - \frac{4}{3NK^2}\frac{C}{\langle e \rangle^2}. \quad (35)$$

In the FSS region the energy $\langle e \rangle \approx -1.9$ varies very little. As a function of K we thus expect to see a minimum in V_L at roughly the point where the specific heat C is maximal. As can be seen in Table V this is indeed the case. Assuming the usual scaling behavior of $K_{min}^{V_L}$ and $\nu = 1$, we obtain from a linear fit $K_c = 0.26329(40)$ with $Q = 0.25$, in perfect agreement with our previous results.

Furthermore, recalling the FSS of the specific-heat maxima, we expect that the minima V_{min} of V_L should scale according to $N(\frac{2}{3} - V_{min}) = b_0 + b_1 \ln L$ with $b_1 \approx 2$. In the semilog plot of Fig. 9 we show the data for $N(\frac{2}{3} - V_{min})$ together with such a fit (with $Q = 0.29$), yielding $b_0 = 4.04(54)$ and $b_1 = 1.74(12)$. In view of the neglected corrections in (35) and the ambiguities in the fits of C_{max}, the agreement with the expectation is quite satisfactory. Similarly to the specific-heat maxima, however, the data can also be fitted with an ansatz $N(\frac{2}{3} - V_{min}) \propto L^{\alpha/\nu}$, yielding $\alpha/\nu = 0.144(10)$ and $Q = 0.43$; see Fig. 9.

IV. RESULTS IN THE DISORDERED PHASE

To supplement the FSS analyses near criticality we have performed further simulations in the disordered phase. Here we concentrated on the approach to criticality of the susceptibility and the specific heat. Most data were obtained from one random lattice with $N = 40\,000$ sites in the inverse temperature range $K = 0.22 - 0.26$; see Table VIII. The quoted autocorrelation times refer to the scale at which the measurements are taken. If this is converted to a Metropolis scale (with the unit of time set to N spin flips) by multiplying with a factor $f = 10\langle |C| \rangle/N$, we obtain $\tau_e \approx 1 - 2$ and $\tau_\chi \approx 0.07$ (apart from the point at $K = 0.260$).

TABLE VII. Maxima of the specific heat, C_{max}, for the Ising model on a regular simple square lattice of size $L \times L$, and the corresponding pseudocritical couplings K_{max}^C, as computed from the exact expressions given in Ref. 41. The numerical errors are of the order ± 1 in the last digit.

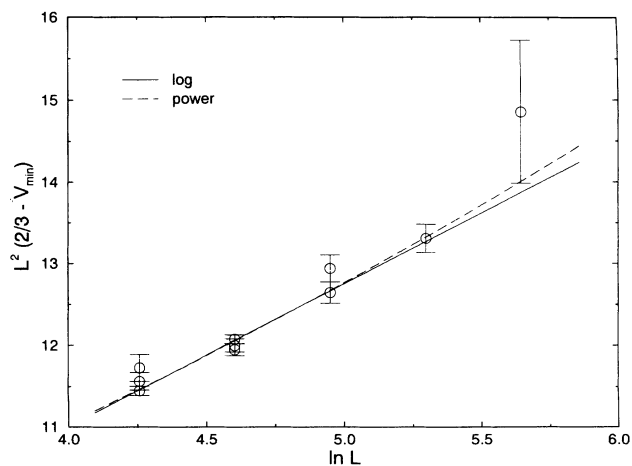| L	K_{max}^C	C_{max}
20	0.433 23	1.6659
40	0.436 85	2.0167
60	0.438 11	2.2200
80	0.438 74	2.3637
100	0.439 12	2.4750
120	0.439 38	2.5657
140	0.439 57	2.6424
160	0.439 71	2.7088
180	0.439 81	2.7673
200	0.439 90	2.8196
220	0.439 97	2.8669
240	0.440 03	2.9101
260	0.440 08	2.9498
280	0.440 12	2.9865
290	0.440 14	3.0039

FIG. 9. Finite-size scaling of the minima V_{min} of the energetic fourth-order parameter V_L. The solid and dashed lines show logarithmic and power-law fits, which are closely related to the corresponding fits to the specific-heat data in Fig. 8 (see text).

TABLE VIII. Results in the disordered phase for a random lattice of $N = 40\,000$ sites.

K	$\hat{\tau}_e$	$\hat{\tau}_\chi$	$\langle e \rangle$	C	$\langle |m| \rangle$	χ	χ_{imp}	χ'
0.220	85(7)	12.8(4)	$-1.208\,11(36)$	0.515(11)	0.018\,850(77)	4.901(35)	4.9825(54)	1.774(14)
0.225	77(6)	11.0(3)	$-1.263\,21(37)$	0.589(13)	0.021\,20(13)	6.354(69)	6.3436(65)	2.311(25)
0.230	67(5)	8.0(2)	$-1.321\,64(33)$	0.648(15)	0.024\,004(88)	8.326(52)	8.337(11)	3.026(19)
0.235	60(4)	6.1(2)	$-1.384\,51(31)$	0.715(16)	0.027\,89(15)	11.44(11)	11.426(14)	4.129(39)
0.240	50(3)	4.06(7)	$-1.452\,04(40$	0.836(12)	0.033\,147(93)	16.550(84)	16.593(29)	6.003(33)
0.245	35(2)	2.61(4)	$-1.525\,11(27)$	0.910(12)	0.041\,10(12)	26.00(15)	26.247(34)	9.447(59)
0.250	24(1)	1.49(2)	$-1.605\,38(31)$	1.077(10)	0.055\,31(11)	47.86(17)	48.006(87)	17.260(63)
0.260	3.30(5)	0.910(7)	$-1.808\,66(10)$	1.8356(70)	0.213\,71(29)	664.7(1.6)	664.2(1.1)	189.71(40)

A. Susceptibilities and exponent γ

To analyze the data for the susceptibilities in Table VIII we have assumed the leading singular behavior as K_c is approached,

$$\chi = A(K_c - K)^{-\gamma} , \tag{36}$$

and performed nonlinear three-parameter fits. On the one hand, this requires K values that are sufficiently far away from K_c to guarantee negligible finite-size effects. On the other hand, they should be sufficiently near to K_c to avoid confluent and analytical correction terms in (36), which are difficult to deal with numerically.[42] Both conditions are nonuniversal and can only be satisfied self-consistently, relying on the goodness of the fits. Alternatively, one may rewrite the ansatz (36) as a function of temperature T, or one can consider χ/K instead of χ. In effect this influences the importance of the analytic correction term and thus the range of K or T values over which the simple ansatz with only the leading singularity can be applied. Our results of goodness-of-fit tests for these different possibilities can be summarized as follows. If we consider $\chi/K = N\langle m^2 \rangle$, $\chi_{\text{imp}}/K = \langle |C| \rangle$, or χ'/K (as in most previous works), then fits to $A(K_c - K)^{-\gamma}$ are self-consistent in an interval $K \in (0.22, 0.25)$. The data at $K = 0.26$ clearly display finite-size effects. The inclusion of the data at $K = 0.22$ seems marginal in the sense that the goodness Q of the fits [or, equivalently, their chi-squared (χ^2)] is still acceptable, but worse than for fits omitting these data. For this reason we give in Table IX the results for both fitting ranges, corresponding to four and three degrees of freedom (DOF), respectively. We see that all estimates for K_c are compatible with our FSS

values of $K_c \approx 0.2630$. As expected the most precise values result from fits to the improved susceptibility, $\chi_{\text{imp}}/K = \langle |C| \rangle$. This is also illustrated in a slightly different way in Fig. 10, where we plot the chi-squared per degree of freedom (χ^2 per DOF) of linear least-squares fits with _fixed_ K_c versus K_c. Actually we have plotted $\sqrt{\chi^2}$ per DOF in order to demonstrate that the chi-squared increases quadratically as K_c is varied around its optimal value.

Regarding the critical exponent γ we observe that the estimates coming from the fits to $\chi/K = N\langle m^2 \rangle$ and $\chi'/K = N(\langle m^2 \rangle - \langle |m| \rangle^2)$ are, within error bars, fully consistent with the regular lattice values of $\gamma = \frac{7}{4} = 1.75$. The results for γ obtained from fits to $\chi_{\text{imp}}/K = \langle |C| \rangle$ overestimate this value by about 3σ. Thus, taking the error estimates at face value, these results are only barely consistent with $\frac{7}{4}$. Since in absolute terms, however, the deviation is only about 1.6%, we have not tried to improve the statistical consistency by doing a more refined error analysis (with correlation effects between parameters taken more properly into account), which usually tends to increase the error bars.

Notice finally that also $\langle |m| \rangle$ can be used to extract the exponent γ, even though this quantity should tend to zero in the infinite volume limit. The point is that, since $\chi = N\langle m^2 \rangle \sim A(K_c - K)^{-\gamma}$, we expect that

$$\langle |m| \rangle = \langle \sqrt{m^2} \rangle \approx \sqrt{\langle m^2 \rangle} \sim a(K_c - K)^{-\gamma/2} ,$$

with an amplitude $a = \sqrt{A/N}$ which vanishes for large N. In fact, a fit in the interval $K \in [0.22, 0.25]$ yields $\gamma = 1.777(36)$ and $a = 0.0012(1)$ (with $Q = 0.41$), con-

TABLE IX. Results of nonlinear three-parameter fits of the susceptibility data in Table VIII to the leading singularity $A(K_c - K)^{-\gamma}$.

Obs	$K = 0.22$–0.250 4 DOF			$K = 0.225$–0.250 3 DOF		
	A	K_c	γ	A	K_c	γ
χ_{imp}/K	0.084\,9(18)	0.262\,81(10) $Q = 0.90$	1.772\,5(76)	0.083\,6(23)	0.262\,88(13) $Q = 0.98$	1.778\,3(99)
χ/K	0.079\,3(73)	0.263\,05(39) $Q = 0.44$	1.795(33)	0.093(12)	0.262\,51(48) $Q = 0.82$	1.741(44)
χ'/K	0.027\,2(28)	0.263\,36(43) $Q = 0.50$	1.816(37)	0.032\,4(45)	0.262\,76(52) $Q = 0.97$	1.757\,48

TABLE X. Results in the disordered phase for a random lattice of $N = 80\,000$ sites.

K	$\hat{\tau}_e$	$\hat{\tau}_\chi$	$\langle e \rangle$	C	$\langle |m| \rangle$	χ	χ_{imp}	χ'
0.252	36(2)	2.2(2)	$-1.638\,93(19)$	1.151(16)	0.044\,70(12)	63.04(31)	63.546(35)	22.77(11)
0.254	29(2)	1.6(2)	$-1.675\,74(21)$	1.223(14)	0.053\,549(91)	90.86(29)	91.424(55)	32.59(11)

sistent with $\sqrt{A/N} = 0.0014(1)$, as follows by inserting $N = 40\,000$ and recalling $A = 0.079(8)$.

B. Specific heat and exponent α

In view of our FSS results in Sec. III, we have assumed that $\alpha = 0$ and tried to confirm this assumption by fits of our specific-heat data to a logarithmic divergence of the form

$$C = A_0 - A_1 \ln(K_c - K) . \tag{37}$$

Using all data from $K = 0.22$ to $K = 0.25$, the results of such a nonlinear three-parameter fit are $A_0 = -1.07(22)$, $A_1 = 0.516(82)$, and $K_c = 0.2657(41)$, with $Q = 0.18$. Omitting the point at $K = 0.22$ we obtain $A_0 = -0.90(25)$, $A_1 = 0.455(89)$, and $K_c = 0.2631(41)$, with $Q = 0.14$. Here we have also tried to include further data from two additional runs at $K = 0.252$ and $K = 0.254$ on a lattice with 80 000 sites, see Table X. For the susceptibility analysis we had to discard this data since, due to the very small error bars on the χ's, the susceptibility fits are much more sensitive. If the $N = 80\,000$ data were taken into account, the goodness-of-fit parameter Q decreased by about two or even several orders of magnitude for fits to χ' and χ or to the more accurate χ_{imp}, respectively. In this data we thus saw either finite-size effects or, more likely, replica fluctuations, or a combination of both. For the specific heat, on the other hand, the relative errors are much bigger, and fits including the $N = 80\,000$ data gave almost identical
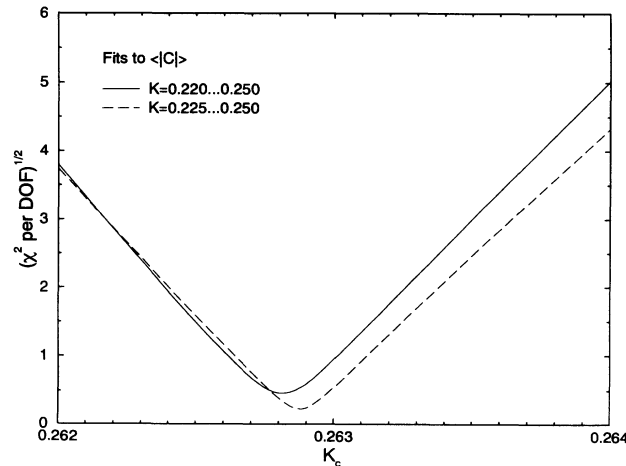
results, with even improved Q values ($A_0 = -1.08(15)$, $A_1 = 0.518(52)$, $K_c = 0.2657(23)$, $Q = 0.36$ for $K \in [0.220, 0.254]$, and $A_0 = -0.99(18)$, $A_1 = 0.489(60)$, $K_c = 0.2647(24)$, $Q = 0.31$ for $K \in [0.225, 0.254]$).

The values for K_c are compatible with, but considerably less accurate than our previous estimates which all gave approximately $K_c = 0.2630$. In the semilog plot of Fig. 11(a) we therefore show C vs $K_c - K$ with $K_c = 0.2630$. The solid straight line is a linear fit of the form (37) with K_c held fixed at its best value. Using all data points with $K \in [0.220, 0.254]$ this yields $A_0 = -0.902(32)$ and $A_1 = 0.4544(82)$, with $Q = 0.28$.

FIG. 10. The chi-squared per degree of freedom (χ^2 per DOF) of least-squares fits with fixed critical coupling K_c to measurements of the improved susceptibility, $\chi_{imp}/K = \langle |C| \rangle$, in the disordered phase. The minima are the best estimates for K_c from these data.
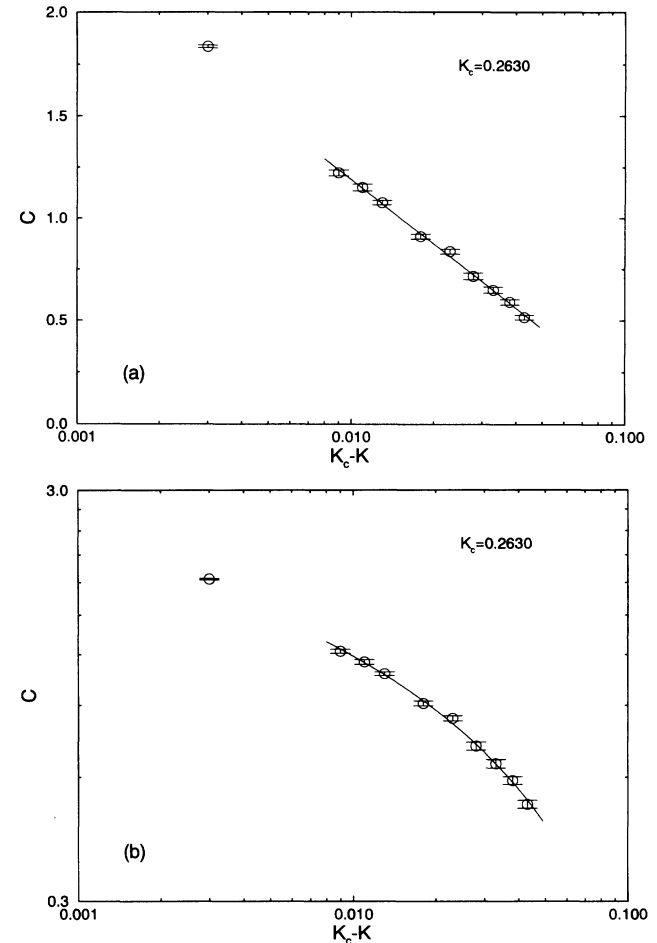

FIG. 11. The specific heat in the disordered phase near the critical coupling K_c. The semilog plot in (a) demonstrates the consistency of our data with a logarithmic scaling behavior. The solid straight line shows a corresponding least-squares fit. In (b) the data and fit displayed in (a) are replotted in a log-log representation. Here a straight line would correspond to a power-law behavior.

The Fig. 11(b) shows the same data and the fit in a log-log representation. Here a pure power law would result in a straight line. Even though this is obviously not the case at $K_c = 0.2630$, fits to a pure power-law ansatz, $C \propto (K_c - K)^{-\alpha}$, with K_c as a free parameter are still acceptable ($Q = 0.26$, for $K \in [0.220, 0.254]$). The parameters, however, then take "unreasonable" values, $K_c = 0.305(18)$ and $\alpha = 1.7(5)$, and the error bars are very large. We also tried to include a constant background term by performing fits to the ansatz $C = a_0 - a_1(K_c - K)^{-\alpha}$, with K_c held fixed at values around 0.2630. This yields α consistent with zero, $\alpha = -0.13(9)$, albeit again with the drawback of huge error bars on all three parameters. Similar to the FSS analysis in Sec. III, also here we cannot really exclude a possible power-law scaling of the specific heat with an exponent $\alpha \neq 0$. We obtain, however, a perfectly consistent picture if we assume logarithmic scaling, that is a value of $\alpha = 0$.

V. CONCLUDING REMARKS

We have performed a fairly detailed analysis of single-cluster Monte Carlo simulations of the Ising model on two-dimensional Poissonian random lattices of Voronoi-Delaunay type. In the first set of simulations at criticality we have applied finite-size scaling methods to various quantities to extract the critical exponents of this model. At first sight our use of different quantities to estimate

the same exponent might appear redundant, since the various estimates are, of course, not independent in a statistical sense. Their consistency, however, gives confidence that corrections to the asymptotic scaling behavior are very small and can safely be neglected. Direct analyses of thermodynamic measurements of the susceptibility in the disordered phase yield compatible results. From both types of simulations the results for the critical exponent α of the specific heat are not really conclusive, but certainly consistent with $\alpha = 0$, i.e., with a logarithmic scaling behavior. On the other hand, from our estimates for the exponents ν, β/ν, γ/ν, and γ, we obtain strong evidence that the Ising model on two-dimensional random lattices behaves qualitatively as on regular lattices, i.e., that (lattice) universality holds for this model.

ACKNOWLEDGMENTS

[1] J. L. Meijering, Philips Res. Rep. **8**, 270 (1953).

[2] R. Collins, Proc. Phys. Soc. **1**, 1461 (1968); and in *Phase Transitions and Critical Phenomena*, edited by C. Domb and M.S. Green (Academic, London, 1972), Vol. 2, p. 271.

[3] J. M. Ziman, *Models of Disorder* (Cambridge University Press, Cambridge, 1976).

[4] C. Itzykson and J.-M. Drouffe, *Statistical Field Theory* (Cambridge University Press, Cambridge, 1989), Vol. 2.

[5] N. H. Christ, R. Friedberg, and T. D. Lee, Nucl. Phys. **B202**, 89 (1982); **B210**, 310 (1982); **B210**, 337 (1982).

[6] C. Itzykson, in *Progress in Gauge Field Theories*, Proceedings of Cargèse Summer School, edited by G. 't Hooft (Plenum, New York, 1983).

[7] R. Friedberg and H.-C. Ren, Nucl. Phys. **B235**, 310 (1984); H.-C. Ren, *ibid.* **B235**, 321 (1984).

[8] F. David and J.-M. Drouffe, Nucl. Phys. B (Proc. Suppl.) **4**, 83 (1988).

[9] C. Moukarzel and H. J. Herrmann, J. Stat. Phys. **68**, 911 (1992).

[10] H. Puhl, Physica A **197**, 14 (1993).

[11] H.-C. Hege, Diploma thesis, FU Berlin, 1984, (unpublished); J. F. McCarthy, Nucl. Phys. **B275**, 421 (1986); W.-Z. Li and J.-B. Zhang, Phys. Lett. B **200**, 125 (1988); H. Koibuchi, Z. Phys. C **39**, 443 (1988); H. Stüben, Diploma thesis, FU Berlin, 1989 (unpublished); H. Stüben, H.-C. Hege, and A. Nakamura, Phys. Lett. B **244**, 473 (1990); J.-B. Zhang and D.-R. Ji, Phys. Lett. A **151**, 469 (1990).

[12] D. Espriu, M. Gross, P. E. L. Rakow, and J. F. Wheater, Nucl. Phys. **B265**, 92 (1986).

[13] M. E. Fisher, J. Math. Phys. **7**, 1776 (1966).

[14] V. S. Dotsenko and V. S. Dotsenko, Adv. Phys. **32**, 129 (1983).

[15] A. B. Harris, J. Phys. C **7**, 1671 (1974).

[16] L. Onsager, Phys. Rev. **65**, 117 (1944).

[17] On a regular square $L \times L$ lattice, the (exponential) autocorrelation time τ_0 of the magnetization grows with the system size as $\tau_0 \propto L^z$ with $z \approx 2.1$–2.2; see D. P. Landau, S. Tang, and S. Wansleben, J. Phys. (Paris) Colloq. **49**, C8-1525 (1988); D. Stauffer, Physica A **184**, 201 (1992); B. Dammann and J. D. Reger, Europhys. Lett. **21**, 157 (1993); C. Münkel, D. W. Heermann, J. Adler, M. Gofman, and D. Stauffer, Physica A **193**, 540 (1993).

[18] R. H. Swendsen and J.-S. Wang, Phys. Rev. Lett. **58**, 86 (1987); J.-S. Wang and R. H. Swendsen, Physica A **167**, 565 (1990).

[19] U. Wolff, Phys. Rev. Lett. **62**, 361 (1989); Nucl. Phys. **B334**, 581 (1990).

[20] R. H. Swendsen, J.-S. Wang, and A. M. Ferrenberg, in *The Monte Carlo Method in Condensed Matter Physics*, edited by K. Binder (Springer, Berlin, 1992), p. 75; C. F. Baillie, Int. J. Mod. Phys. C **1**, 91 (1990); A. D. Sokal, in *Quantum Fields on the Computer*, edited by M. Creutz (World Scientific, Singapore, 1992), p. 211; and (unpublished).

[21] A. M. Ferrenberg and R. H. Swendsen, Phys. Rev. Lett. **61**, 2635 (1988); **63**, 1658(E) (1989).

[22] K. Binder, in *Phase Transitions and Critical Phenomena*, edited by C. Domb and M. S. Green (Academic, New York, 1976), Vol. 5B, p. 1; and in *Monte Carlo Methods in Statistical Physics*, edited by K. Binder (Springer, New York, 1979), p. 1; M. E. Barber, in *Phase Transitions and Critical Phenomena*, edited by C. Domb and J. L. Lebowitz (Academic, New York,

1983), Vol. 8, p. 145; see also the articles in *Finite-Size Scaling and Numerical Simulations of Statistical Systems,* edited by V. Privman (World Scientific, Singapore, 1990).

[23]A brief summary was already given in W. Janke, M. Katoot, and R. Villanova, Phys. Lett. B **315**, 412 (1993).

[24]G. Le Caër and J. S. Ho, J. Phys. A **23**, 3279 (1990).

[25]J.-M. Drouffe and C. Itzykson, Nucl. Phys. **B235**, 45 (1984).

[26]U. Wolff, Phys. Lett. B **228**, 379 (1989).

[27]C. F. Baillie and P. D. Coddington, Phys. Rev. B **43**, 10 617 (1991).

[28]P. Tamayo, R. C. Brower, and W. Klein, J. Stat. Phys. **58**, 1083 (1990).

[29]J.-S. Wang, Physica A **164**, 240 (1990).

[30]M. Hasenbusch and S. Meyer, Phys. Lett. B **241**, 238 (1990).

[31]W. Janke, Phys. Lett. A **148**, 306 (1990).

[32]N. Madras and A. D. Sokal, J. Stat. Phys. **50**, 109 (1988); see also Sokal (Ref. 20).

[33]D. W. Heermann and A. N. Burkitt, Physica A **162**, 210 (1990).

[34]R. G. Miller, Biometrika **61**, 1 (1974); B. Efron, *The Jackknife, the Bootstrap and other Resampling Plans* (SIAM, Philadelphia, PA, 1982).

[35]K. Binder, Z. Phys. B **43**, 119 (1981).

[36]A. M. Ferrenberg and D. P. Landau, Phys. Rev. B **44**, 5081 (1991).

[37]For recent reviews see, e.g., *Dynamics of First Order Phase Transitions,* edited by H. J. Herrmann, W. Janke, and F. Karsch (World Scientific, Singapore, 1992).

[38]K. Binder and D. P. Landau, Surf. Sci. **151**, 409 (1985).

[39]W. H. Press, B. P. Flannery, S. A. Teukolsky, and W. T. Vetterling, *Numerical Recipes—the Art of Scientific Computing* (Cambridge University Press, Cambridge, 1986).

[40]W. Janke (unpublished).

[41]A. E. Ferdinand and M. E. Fisher, Phys. Rev. **185**, 832 (1969).

[42]See, e.g., the discussion in C. Holm and W. Janke, Phys. Rev. B **48**, 936 (1993).